The Integrated Relativistic Iron Line from Active Galactic Nuclei: Chasing the Spin Evolution of Supermassive Black Holes

D. R. Ballantyne

Center for Relativistic Astrophysics, School of Physics, Georgia Institute of Technology, Atlanta, GA 30332

david.ballantyne@physics.gatech.edu

ABSTRACT

The spin of a supermassive black hole (SMBH) is directly related to the radiative efficiency of accretion on to the hole, and therefore impacts the amount of fuel required for the black hole to reach a certain mass. Thus, a knowledge of the SMBH spin distribution and evolution is necessary to develop a comprehensive theory of the growth of SMBHs and their impact on galaxy formation. Currently, the only direct measurement of SMBH spin is through fitting the broad Fe Kα line in AGNs. The evolution of spins could be determined by fitting the broad line in the integrated spectra of AGNs over different redshift intervals. The accuracy of these measurements will depend on the observed integrated line strength. Here, we present theoretical predictions of the integrated relativistic Fe Kα line strength as a function of redshift and AGN luminosity. The equivalent widths of the integrated lines are much less than 300 eV. Searches for the integrated line will be easiest for unobscured AGNs with 2–10 keV luminosities between $44 < \log L_X \leq 45$. The total integrated line makes up less than 4% of the X-ray background, but its shape is sensitive to the average SMBH spin. By following these recommendations, future *International X-ray Observatory* surveys of broad Fe Kα lines should be able to determine the spin evolution of SMBHs.

Subject headings: galaxies: active — galaxies: nuclei — galaxies: Seyfert — surveys — X-rays: diffuse background — X-rays: galaxies

1. Introduction

In astrophysics, black holes can be described by only two parameters: their mass $M_{\rm BH}$ and their angular momentum J (parametrized by the dimensionless spin parameter

$a \equiv cJ/GM_{\rm BH}^2$ where $0 \leq a \leq 1$). Over the last several decades, estimates of black hole masses have been obtained by measuring the gravitational influence of the hole on nearby objects such as binary stellar companions (e.g., Bolton 1972; Cowley et al. 1983; McClintock & Remillard 2006), orbiting stars (e.g., Ghez et al. 2008), stellar cusps (e.g., Magorrian et al. 1998) or dense clouds of ionized gas (e.g., Peterson et al. 2004). However, measurements of black hole spin are much more difficult to obtain as the spin only significantly affects the shape of space-time out to $\approx 6\ r_g$ ($r_g = GM_{\rm BH}/c^2$ is a gravitational radius) from the event horizon (Bardeen et al. 1972). In particular, the value of the spin is directly related to the radius of the innermost stable circular orbit (ISCO) around the hole (Bardeen et al. 1972), and therefore impacts the radiative efficiency of thin accretion disks. If the accretion flow is rotating in the same sense as the hole, then a larger a brings the ISCO closer to the event horizon, increasing the efficiency that an accretion flow can convert gravitational potential energy into radiation. A larger fraction of the rest-mass energy is radiated away in a highly efficient accretion disk, reducing the growth rate of the black hole mass. Therefore, measuring the distribution of spins will elucidate the role of steady accretion (e.g., Volonteri et al. 2005), chaotic accretion (e.g., King & Pringle 2006) and black hole mergers (e.g., Berti & Volonteri 2008) in the build-up of supermassive black holes (SMBHs).

X-ray variability and optical microlensing data show that the X-ray source in AGNs is within 10 r_g (e.g., Iwasawa et al. 2004; Dai et al. 2010), indicating that the accretion disk is likely illuminated by X-rays down to the ISCO. As spin clearly impacts the radius of the ISCO, the extent of the red wing of the relativistically broadened Fe Kα line is a direct measurement of black hole spin (e.g., Reynolds & Fabian 2008). In recent years, long observations by *XMM-Newton* and *Suzaku* have used this method to obtain SMBH spin estimates for a small number of bright, nearby Seyfert 1 galaxies (Brenneman & Reynolds 2006; Miniutti et al. 2009; Schmoll et al. 2009). These type of spin measurements depend on precise spectral fitting to the broad Fe Kα line and continuum and are most easily performed on sources with strong Fe Kα lines. Thus, the larger collecting area provided by the future *International X-ray Observatory* (*IXO*) will be necessary in order to extend these types of spin measurements over a significant range of redshift. In the meantime, attempts have been made to measure the average Fe Kα line profile by stacking the X-ray data of the many AGNs detected in deep *Chandra* or *XMM-Newton* surveys over a wide range of redshift and AGN luminosity. If a significant Fe Kα signal can be detected in the integrated spectrum then, in principle, the average spin of the black holes contributing to the line could be determined. Again, the ability to make this measurement depends crucially on the strength of the integrated Fe Kα line. Streblyanska et al. (2005) averaged the *XMM-Newton* spectra of type 1 and type 2 AGNs detected in the Lockman Hole and found a strong (equivalent width [EW] $\sim$ 500 eV) and broad Fe Kα line that indicated a non-zero spin for

the average SMBHs in their sample. However, similar stacking analyses of different datasets by Brusa et al. (2005) and Corral et al. (2008) were not able to detect a broad component, with Corral et al. (2008) finding that the EW of the broad component must be < 400 eV. These attempts to measure the integrated broad Fe Kα line are technically challenging and are limited by the unknown intrinsic distribution of broad Fe Kα line strengths.

Recently, Ballantyne (2010) described a method by which the average EW of the broad Fe Kα line could be calculated as a function of z and luminosity. That paper concentrated on the distribution of likely EWs from individual sources, and did not consider the result of integrating lines over specific redshift intervals, a step crucial to measuring the spin evolution of SMBHs. This letter builds on the Ballantyne (2010) method to calculate the integrated Fe Kα line over several different redshift and luminosity ranges. We also consider the dependence of AGN obscuration on the appearance of the integrated Fe Kα lines. These predictions show which regions in the redshift and AGN luminosity plane will have the largest average broad Fe Kα EW, and will be vital for guiding current and future attempts to map out the spin evolution of SMBHs by fitting the average Fe Kα line profile. The calculations are reviewed in the next section, and the results are presented in Sect. 3. The following Λ-dominated cosmology is assumed in this paper: $H_0 = 70$ km s^{-1} Mpc^{-1}, $\Omega_\Lambda = 0.7$, and $\Omega_m = 0.3$ (Spergel et al. 2003).

2. Calculations

The calculation of the mean Fe Kα EW as a function of z and AGN 2–10 keV luminosity, L_X, broadly follows the procedure described by Ballantyne (2010). The Ueda et al. (2003) hard X-ray luminosity function (HXLF) is combined with the observed AGN black hole mass function (BHMF) at $z = 0.15$ (Netzer 2009) to calculate an Eddington ratio distribution at a given L_X. In order to predict the integrated Fe Kα line over several cosmologically interesting redshift ranges we assume that the BHMF evolves as $(1 + z)^{1.64}$ between $z = 0$ and 5 (Labita et al. 2009). It is also assumed that the broad Fe Kα line is produced by a single strong reflection event from a dense, geometrically thin accretion disk that can be approximated by a constant density slab (Ross & Fabian 1993; Ballantyne et al. 2001). The EW of the iron line depends on the photon index of the illuminating power-law Γ, the relative abundance of iron $A_{\rm Fe}$, the ionization parameter of the disk ξ, and the reflection fraction, R, which determines the relative strength of the reflected spectrum in the total observed spectrum (Ballantyne et al. 2002). The first three of these parameters are known to depend on the Eddington ratio of the AGN (Netzer & Trakhtenbrot 2007; Inoue et al. 2007; Risaliti et al. 2009). Reflection spectra are then computed for each Eddington ratio

contributing to an observed L_X. The Fe Kα EW is measured for each spectrum (assuming $R = 0.5$, 1, 2 or 4) and averaged over the Eddington ratio distribution to give a single value for that L_X. In order for the integrated line to reflect the changes in ξ and Γ, we keep track of the average energy at which the Fe Kα line reaches a maximum $\langle E_{\rm max} \rangle$. These calculations are performed for 100 values of L_X between $\log L_X = 41.5$ and $\log L_X = 48$, and for 100 values of z between $z = 0$ and 5.

These results can now be included in a X-ray background (XRB) synthesis calculation to predict the strength and profile of the integrated broad Fe Kα line over several different ranges of luminosity and redshift. The synthesis model used here was last described by Draper & Ballantyne (2009), although we neglect the contribution of blazars for this application. The integrated rest-frame spectral intensity $I(E)$ are computed by evaluating:

$$I(E) = \frac{c}{H_0} \int_{z_{\rm min}}^{z_{\rm max}} \int_{\log L_X^{\rm min}}^{\log L_X^{\rm max}} \frac{d\Phi(L_X, z)}{d \log L_X} \frac{S_E(L_X, z) d_l^2}{(1+z)^2 (\Omega_m (1+z)^3 + \Omega_\Lambda)^{1/2}} d \log L_X dz, \qquad (1)$$

where $d\Phi(L_X, z)/d \log L_X$ is the Ueda et al. (2003) HXLF, $S_E(L_X, z)$ is the absorbed rest-frame spectrum of an AGN with intrinsic luminosity L_X at redshift z, and d_l is the luminosity distance to redshift z. At each (L_X, z) pair in the integral, a relativistically broadened Fe Kα line appropriate for a maximally-spinning (i.e., $a \sim 1$) SMBH is added to the spectrum S_E such that it has the EW predicted by the reflection calculations described above. The relativistic profile for the line was calculated using the 'laor2' model in XSPEC12 (Laor 1991; Arnaud 1996) with a line emissivity of 0 between 1.2 and 6 r_g and -3 from 6 to 400 r_g (cf., Nandra et al. 2007). The inclination angle of the line emitting material was taken to be 30 degrees, and the rest energy of the line is set to $\langle E_{\rm max} \rangle$ to account for changes in the average ionization state of the line as L_X and z are varied. Finally, to be consistent with the calculation of the Fe Kα lines, the photon index of $S_E(L_X, z)$ is derived from averaging Γ over the Eddington ratio distribution for a given (L_X, z) pair. This method translates to average photon indices varying from 1.4 to 2.5 depending on the value of z or L_X. In practice, this method of determining Γ for $S_E(L_X, z)$ has a negligible effect on the results.

The integrated AGN spectra are then computed for five different redshift ranges: $0 \leq z \leq 5$, $0 \leq z \leq 1$, $1 < z \leq 2$, $2 < z \leq 3$ and $3 < z \leq 5$. For each redshift range, five intervals in luminosity are considered: $41.5 \leq \log L_X \leq 43$, $43 < \log L_X \leq 44$, $44 < \log L_X \leq 45$ and $45 < \log L_X \leq 48$. The EW of the Fe Kα line is measured by directly integrating the resulting spectra. The EW measurements are performed separately for type 1 AGNs (those with hydrogen column densities $\log N_{\rm H} < 22$) and type 2 AGNs (those with $22 \leq \log N_{\rm H} \leq 25$), although the EW of the broad line in this model is independent of the obscuration toward the AGN. The impact of obscuration will be discussed at the end of Sect. 3.1.

3. Results

3.1. Integrated EWs

Figure 1 plots the measured EWs from the integrated spectra described in the previous section. The solid lines show the results for $R = 1$ while the dashed and dotted lines assume $R = 2$ and 0.5, respectively. The colors denote the different redshift ranges over which the integration was performed. The measured EWs in all cases are significantly less than 400 eV, consistent with the upper-limit derived by Corral et al. (2008). Indeed, for $R = 1$, the EWs are between $\sim$ 90 eV and $\sim$ 220 eV. In fact, even if $R = 2$ for every AGN, the EW of the integrated Fe Kα line does not break 320 eV. If the average R of AGNs is closer to 0.5 then the majority of the integrated broad lines have EWs$<$ 120 eV.

In the model of Fe Kα production described here and by Ballantyne (2010) the EW of the line is ultimately a function of the Eddington ratio of the AGN. If the SMBH is accreting too weakly, there is no optically thick disk for reflection to occur (Narayan & Yi 1995). In the opposite extreme, if the accretion ratio is very close to the Eddington limit there is also little observed reflection signature because the disk is very highly ionized (Ballantyne et al. 2002). The strongest Fe Kα line arises from recombination onto He-like iron, but this occurs over a relatively narrow range of ionization parameter (Ballantyne et al. 2002), and, therefore, a correspondingly small range of Eddington ratios (Ballantyne 2010). This interplay between Eddington ratios and Fe Kα EWs is reflected in the redshift distributions of the integrated EW seen in Figure 1. For all AGNs with $\log L_X < 45$ the largest integrated EW is found from those with $z < 1$. As z increases, the average mass of active SMBHs increases, which, at a constant L_X, corresponding to a decreasing Eddington ratio. Therefore, the integrated Fe Kα EW drops as z increases because a larger fraction of AGNs at these luminosities are accreting too weakly to produce a strong disk line. Integrating over the entire redshift range (black lines in Fig. 1) results in a weighted average of this behavior. In contrast, the Fe Kα EWs of AGNs with $\log L_X > 45$ are largest for $1 < z \leq 2$ and smallest for $z < 1$. The luminosities of these AGNs are large enough that ionized Fe Kα lines contribute significantly at $z > 1$ and boost the integrated EW. In this case, the Eddington ratios at lower z are, on average, too large and the resulting disk lines are weaker. At larger redshifts, the increasing SMBH mass reduces the average Eddington ratio which results in strong neutral Fe Kα emission. This discussion illustrates that, for a fixed luminosity range, the integrated line probes smaller Eddington ratios as the redshift increases. Elucidating the spin evolution of the SMBH population over a fixed interval of mass will require measuring the integrated Fe Kα line over ranges of progressively higher luminosity as the redshift increases.

At face value, the results of Fig. 1 indicate that experiments using the broad Fe Kα

line to measure the spin evolution of SMBHs should be targeted toward integrating the spectra of AGNs with $\log L_X > 45$, as these sources are the ones predicted to have the strongest integrated EWs. The difficulty with this strategy is that such AGNs are rare at all redshifts (e.g., Ueda et al. 2003), and thus the compilation of suitable samples will be extremely problematic even with the enhanced sensitivity of *IXO*. Therefore, we conclude that AGNs with $44 < \log L_X \leq 45$ will provide the best sample to search for the integrated broad Fe Kα line. These AGNs are close to the knee of the HXLF at all redshifts (e.g., Ueda et al. 2003) and will therefore be common enough to provide a useful sample at several different redshift bins. The broad lines from these AGNs will show a mixture of of neutral and ionized reflection with $\langle E_{\rm max} \rangle \approx 6.5$–$6.6$ keV.

Examples of the integrated $R = 1$ spectra in the $44 < \log L_X \leq 45$ range are shown as solid lines in Figure 2 with the colors denoting the redshift ranges as in fig. 1. These spectra were calculated assuming that the Fe Kα line was being emitted all the way down to the ISCO of a maximally spinning black hole. The dashed lines show the integrated spectra if the ISCO is at 6 r_g, as would be the case for a non-spinning black hole. As expected, this scenario causes the integrated line to be slightly less broad and more peaked. This small difference in the line profile should be measurable if a large enough sample of AGNs could be included in the integral. This result nicely illustrates the importance of targeting AGN in the luminosity range that will produce the most intense integrated broad Fe Kα line.

The integrated spectra shown in figure 2 and the associated EWs plotted in fig. 1 are compiled from only type 1 AGNs. The dotted blue line in Fig. 2 plots the integrated type 2 spectrum with $44 < \log L_X \leq 45$ and $z \leq 1$. Our calculations assume that there is no difference in the broad Fe Kα EW between the type 1 and 2 AGNs. However, a visual inspection of the type 2 spectrum in fig. 2 seems to indicate a much more intense broad Fe Kα line. Indeed, performing the same integration of the type 2 line gives an EW of 460 eV as compared to 180 eV for the type 1 AGN. The strong absorption in the average type 2 spectrum causes the continuum to curve downwards at energies < 5 eV and enhances the Fe K edge at 7.1 keV. These effects conspire to artificially enhance the EW of the broad Fe Kα line. Therefore, unless the underlying spectrum and absorption distribution is well known, the search for broad Fe Kα lines in integrated spectra should only be performed on unobscured, type 1 AGNs.

3.2. The Broad Line in the X-ray Background

Performing the integral of eqn. 1 over all z and $\log L_X$, but now redshifting S_E into the observed frame results in a prediction of the contribution of the Fe Kα line to the entire XRB.

Other authors have made similar predictions (Gilli et al. 1999; Gandhi & Fabian 2003), but have had to make very simple assumptions on the Fe Kα strength and shape. Figure 3 shows the first prediction of the Fe Kα contribution to the XRB that arises from a physical model of the Fe Kα line distribution. This figure plots the ratio of the XRB spectrum including the broad line to one which does not include the broad line. Predictions are shown for $R = 1$ (solid line), 2 (short-dashed line) and 4 (dot-dashed line). The long-dashed line plots the ratio for a model where the broad line has a constant EW of 100 eV and results from neutral reflection. In all of these cases the line is broadening using the 'laor2' model as described in Sect. 2, except for the dotted line which plots the $R = 1$ model with all lines arising from 6 r_g (also using the 'laor' model).

Figure 3 shows that the maximum contribution of the broad Fe Kα line to the XRB is 6%, but, since intense reflection cannot be a common occurrence in AGNs (Gandhi et al. 2007; Ballantyne 2010), the contribution is more realistically much less than 4%. These values are in agreement with the previous predictions of Gilli et al. (1999) and Gandhi & Fabian (2003). The contribution of integrating multiple observed-frame spectra and relativistic blurring smears the Fe Kα contribution over 6 keV in energy, but there is a slight difference between the profiles with different spin distributions. Therefore, given a very high quality spectrum of the X-ray background, the total integrated Fe Kα profile will be able to determine the average spin of SMBHs over cosmic time.

4. Conclusions

Measurements of the spin distribution of SMBHs will have profound consequences on our understanding of galaxy formation and evolution. The only direct way to measure SMBH spins is via the broad Fe Kα line in AGNs, and attempts have been made to measure the Fe Kα profile in the spectrum of AGNs that have been integrated over a range of z and $\log L_X$. The accuracy and precision of these measurements will be maximized if the spectral fitting can be performed on Fe Kα lines with the largest possible EW. Therefore, this letter presented predictions of the integrated relativistic Fe Kα EW as functions of z and $\log L_X$. Fig. 1 showed that the integrated broad Fe Kα EW will be significantly less than 300 eV for all ranges of z and $\log L_X$. In fact, if $R = 1$ for most AGNs, the integrated broad component will have an EW between 100 and 200 eV. Taking into account the relative space density of AGNs, it is recommended that the search for integrated broad Fe Kα lines be confined to AGNs with luminosities in the range $44 \leq \log L_X < 45$. It is further recommended that these experiments be limited to type 1 AGNs.

Stepping back from the quantitative results, this letter has shown that measuring the

spin evolution of SMBHs can be done with the broad Fe Kα line. In fact, *IXO* will be perfectly placed to obtain this goal, as its sensitivity will allow it to obtain the high-quality spectra necessary to measure the broad Fe Kα lines. *IXO* spectral surveys of target lists provided by the *Chandra* deep fields will be a very powerful tool to trace the spin of SMBHs up to and beyond $z = 1$.

The referee is acknowledged for a detailed and useful report that greatly improved the paper.

REFERENCES

Arnaud, K.A., 1996, Astronomical Data Analysis Software and Systems V, eds. Jacoby G. and Barnes J., p17, ASP Conf. Series Vol 101

Ballantyne, D.R., 2010, ApJ, 708, L1

Ballantyne, D.R., Ross, R.R. & Fabian, A.C., 2001, MNRAS, 327, 10

Ballantyne, D.R., Fabian, A.C. & Ross, R.R., 2002, MNRAS, 329, L67

Bardeen, J.M., Press, W.H. & Teukolsky, S.A., 1972, ApJ, 178, 347

Berti, E. & Volonteri, M., 2008, ApJ, 684, 822

Bolton, C.T., 1972, Nature, 235, 271

Brenneman, L.W. & Reynolds, C.S., 2006, ApJ, 652, 1028

Brusa, M., Hilli, R. & Comastri, A., 2005, ApJ, 621, L5

Corral, A. et al., 2008, A&A, 492, 71

Cowley, A.P., Crampton, D., Hutchings, J.B., Remillard, R. & Penfold, J.E., 1983, ApJ, 272, 118

Dai, X., Kochanek, C.S., Chartas, G., Kozłowski, S., Morgan, C.W., Garmire, G. & Agol, E., 2010, ApJ, 709, 278

Draper, A.R. & Ballantyne, D.R., 2009, ApJ, 707, 778

Fabian, A.C., Rees, M.J., Stella, L. & White, N.E., 1989, MNRAS, 238, 729

Gandhi, P. & Fabian, A.C., 2003, MNRAS, 339, 1095

Gandhi, P., Fabian, A.C., Suebsuwong, T., Malzac, J., Miniutti, G., Wilman, R.J., 2007, MNRAS, 382, 1005

Ghez, A., et al., 2008, ApJ, 689, 1044

Gilli, R., Comastri, A., Brunetti, G. & Setti, G., 1999, New A, 4, 45

Inoue, H., Terashima, Y., & Ho, L.C., 2007, ApJ, 662, 860

Iwasawa, K., Miniutti, G. & Fabian, A.C., 2004, MNRAS, 355, 1073

King, A.R. & Pringle, J.E., 2006, MNRAS, 373, L90

Labita, M., Decarli, R., Treves, A. & Falomo, R., 2009, MNRAS, 399, 2099

Laor, A., 1991, ApJ, 376, 90

Magorrian, J. et al., 1998, AJ, 115, 2285

McClintock, J.E. & Remillard, R.A., 2006, in Compact Stellar X-ray Sources, ed. W.H.G. Lewin & M. van der Klis, pp. 157-214. Cambridge: Cambridge Univ

Miniutti, G., Panessa, F., de Rosa, A., Fabian, A.C., Malizia, A., Molina, M., Miller, J.M. & Vaughan, S., 2009, MNRAS, 398, 255

Nandra, K., O'Neill, P.M., George, I.M., & Reeves, J.N. 2007, MNRAS, 382, 194

Narayan, R. & Yi, I., 1995, ApJ, 452, 710

Netzer, H., 2009, ApJ, 695, 793

Netzer, H. & Trakhtenbrot, B., 2007, ApJ, 654, 754

Peterson, B.M., et al., 2004, ApJ, 613, 683

Reynolds, C.S. & Fabian, A.C., 2008, ApJ, 675, 1048

Risaliti, G., Young, M. & Elvis, M., 2009, ApJ, 700, L6

Ross, R.R. & Fabian, A.C., 1993, MNRAS, 261, 74

Schmoll, S., Miller, J.M., Volonteri, M., Cackett, E., Reynolds, C.S., Fabian, A.C., Brenneman, L.W., Miniutti, G. & Gallo, L.C., 2009, ApJ, 703, 2171

Spergel, D.N., et al., 2003, ApJS, 148, 175

Streblyanska, A., Hasinger, G., Finoguenov, A., Barcons, X., Mateos, S. & Fabian, A.C., 2005, A&A, 432, 395

Ueda, Y., Akiyama, M., Ohta, K. & Miyaji, T., 2003, ApJ, 598, 886

Volonteri, M., Madau, P., Quateart, E. & Rees, M.J., 2005, ApJ, 620, 69

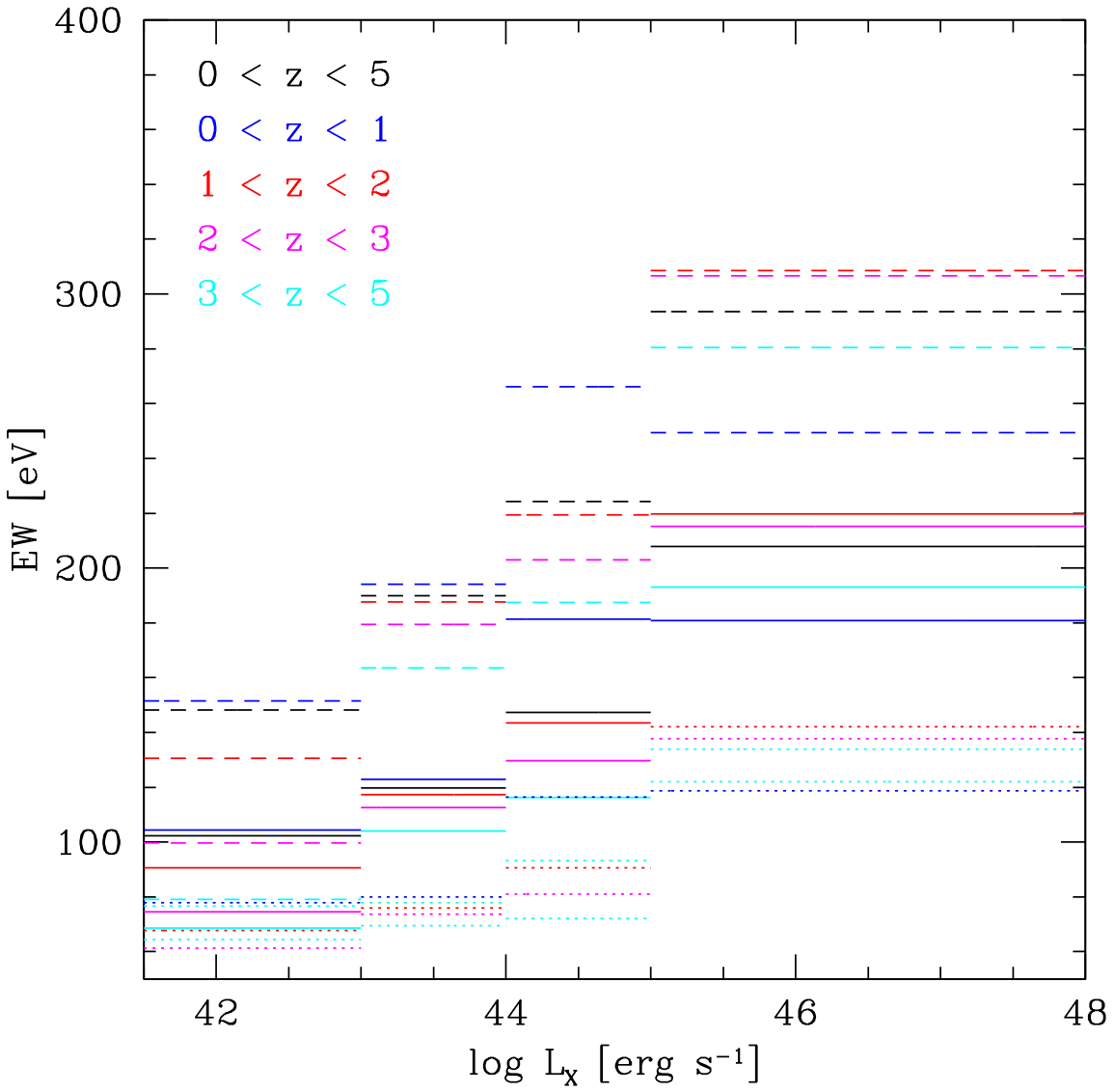

Fig. 1.— Fe Kα EWs measured from AGN spectra integrated over different ranges of z and L_X (Eqn. 1). The colors denote the different redshift ranges the integrals were performed over with black indicating the result from the entire $z = 0$ to 5 interval. The solid lines show the results for a reflection fraction of unity (i.e., $R = 1$), while the dashed and dotted lines plot the EWs if all AGNs have $R = 2$ or 0.5, respectively.

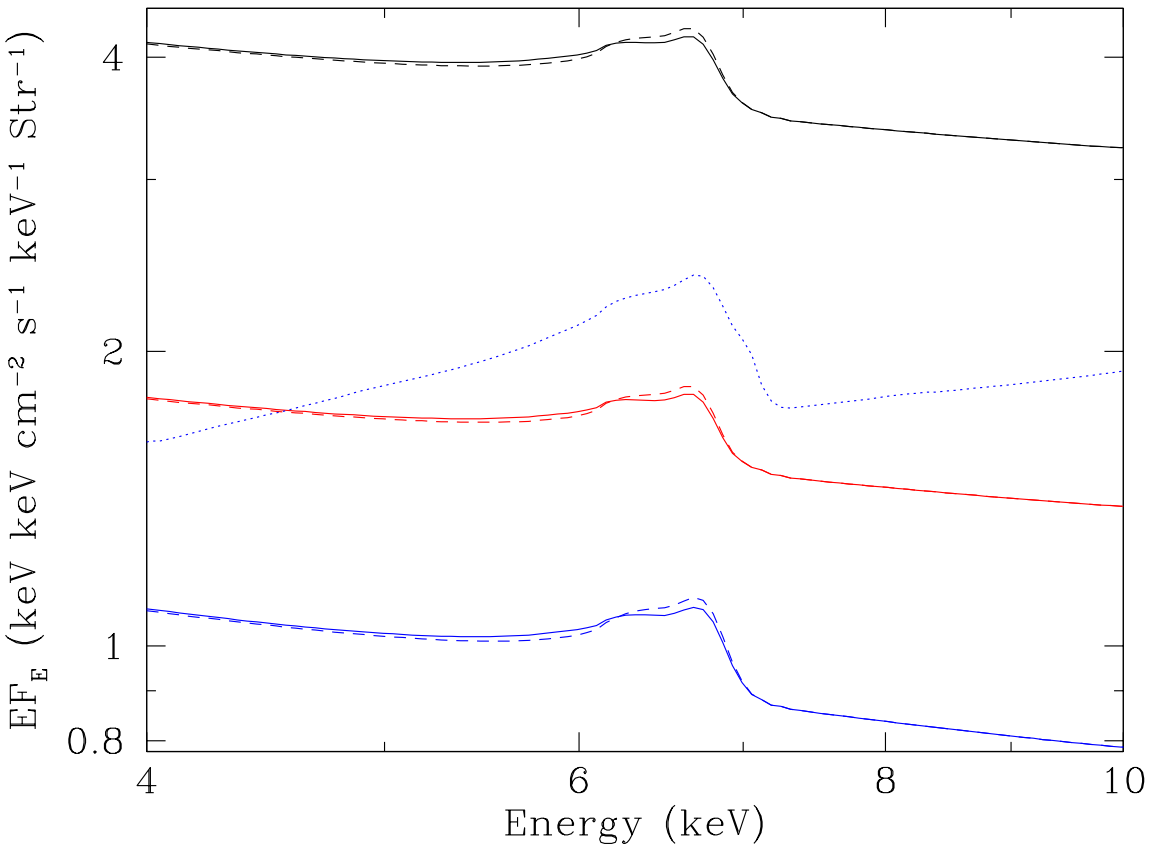

Fig. 2.— Examples of the integrated $R = 1$ spectra from which the Fe Kα EWs were measured. The colors correspond to the same redshift ranges as in Fig. 1. The solid lines show the spectra for the $44 < \log L_X \leq 45$ bin assuming the emission line extends down to the ISCO of a rapidly spinning black hole. The dashed lines plot the same spectra, but now assuming that the ISCO is 6 r_g for all AGNs. Both the solid and dashed lines are the integrated spectra including only type 1 AGNs (i.e., those with $\log N_{\rm H} < 22$). The dotted blue line plots the integrated type 2 spectrum for AGNs with $44 < \log L_X \leq 45$ and $z \leq 1$. The lines in this spectrum also assume emission down the ISCO of a rapidly spinning black hole. In our model the EW of the broad Fe Kα line is independent of nuclear obscuration.

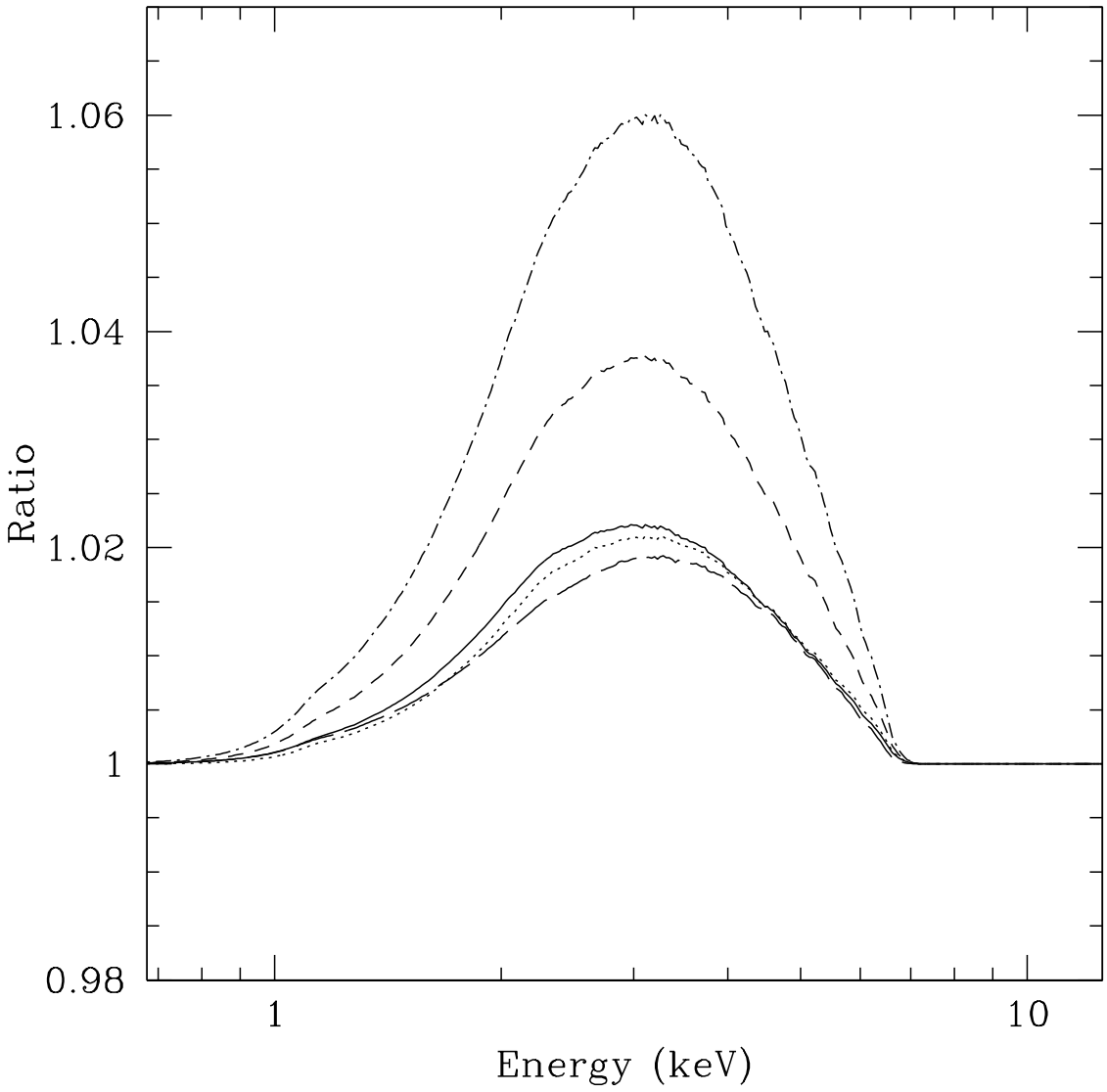

Fig. 3.— The ratio of a model XRB spectrum that includes the broad Fe Kα line to one that does not include the broad line. The ratios shown include a model with $R = 1$ (solid line), $R = 2$ (short-dashed line) and $R = 4$ (dot-dashed line). Also shown is the ratio from a model where each AGN has a neutral broad Fe Kα with a constant EW of 100 eV (long-dashed line). Finally, the dotted line corresponds to a $R = 1$ model where all the SMBHs are non-spinning and the lines extend to only 6 r_g.